

SILICEOUS SINTER DIAGENESIS AT THE OPAL MOUND, ROOSEVELT HOT SPRINGS, UTAH, USA

B.Y. LYNNE¹, K.A. CAMPBELL¹, J. MOORE² & P.R.L. BROWNE¹

¹Department of Geology, University of Auckland, Private Bag 92019, Auckland, New Zealand

²University of Utah, Energy and Geoscience Institute, Salt Lake City, Utah, USA

SUMMARY - Siliceous sinter from the Opal Mound at Roosevelt Hot Springs preserves a complete diagenetic continuum from opal-A to quartz. Sinters from vent, near-vent and mid- and distal-apron environments were studied. ¹⁴C AMS dating yielded ages of 1900 years BP for a sample of quartz mineralogy and 1600 years BP for a distal slope sample with opal-A/CT mineralogy. The transformation from opal-A to quartz in the near-vent sample is more rapid than in sinter deposits of the Taupo Volcanic Zone, New Zealand, which take as long as 40,000 years to transform to diagenetic quartz. Two generations of quartz occur at Opal Mound, diagenetic and hydrothermal quartz. Diagenetic quartz is identified by the presence of moganite, and equant, blocky nanocrystals of opal-C incorporated into quartz crystals growing parallel to the sinter surface. Hydrothermal vein quartz infills fractures with crystals that grow perpendicular to the sinter surface and do not contain moganite. Conductive heat transfer from the injection of thermal fluids that deposited vein quartz in fractures may be responsible for accelerating diagenesis at Opal Mound.

1. INTRODUCTION

Siliceous sinter is common in thermal regions as subaerial hot spring deposits. Where near-neutral alkali chloride fluids discharge at the surface and cool below 100 °C, silica precipitates to deposit siliceous sinter (Fournier and Rowe, 1966). Initially the silica occurs as a non-crystalline opal-A deposit on all available substrates; hence, sinters are paleoenvironmentally significant. Biotic and abiotic inclusions (e.g., plants, microbes, rock fragments) can become entombed, silicified and fossilised. Over time, opal-A transforms into opal-CT ± opal-C ± moganite and eventually to quartz (White *et al.*, 1964, Smith, 1998, Herdianita *et al.*, 2000a, Campbell *et al.*, 2001, Lynne and Campbell, 2003, 2004). This maturation process involves a loss of water and mineralogical and morphological changes at macro- and microstructural scales (Lynne and Campbell, 2004). Depositional and post-depositional conditions, such as weathering or heating related to spring discharges or fumarolic activity also affect rates of diagenetic transformation and the preservation potential of the sinter (Lynne and Campbell, 2004). Therefore an understanding of diagenesis is necessary to reconstruct paleoenvironmental conditions in hot spring settings.

2. GEOLOGICAL SETTING

Roosevelt Hot Springs is the amongst the hottest and best documented of the geothermal resources in the Basin and Range Province, of the western U.S.A. The field is located on the eastern edge of the Province in south central Utah (Fig. 1), on the western margin of the Mineral Mountains. The geothermal field covers ~32km². The reservoir is developed in fractured Precambrian gneiss and Tertiary granite (Nielson *et al.*, 1978). Fluid flow is controlled by steeply dipping north- and east-trending normal faults that cut older low-angle normal faults. Temperatures as high as 268 °C have been measured (Capuano and Cole, 1982). Large sinter deposits occur at the northern and southern ends of the north-trending Opal Mound fault, which appears to mark the western boundary of the reservoir. Moore and Nielson (1994) recognised two generations of sinter at the Opal Mound; an early generation of white vitreous sinter and a younger generation of thinly banded and red, yellow, orange and colourless sinter marginal to the older deposits. Although sinter deposits are associated with many geothermal systems in the Basin and Range Province, extensive sheets of coloured metal-rich sinter are found only at Roosevelt Hot Springs and Steamboat Hot Springs in Nevada (White *et al.*, 1964).

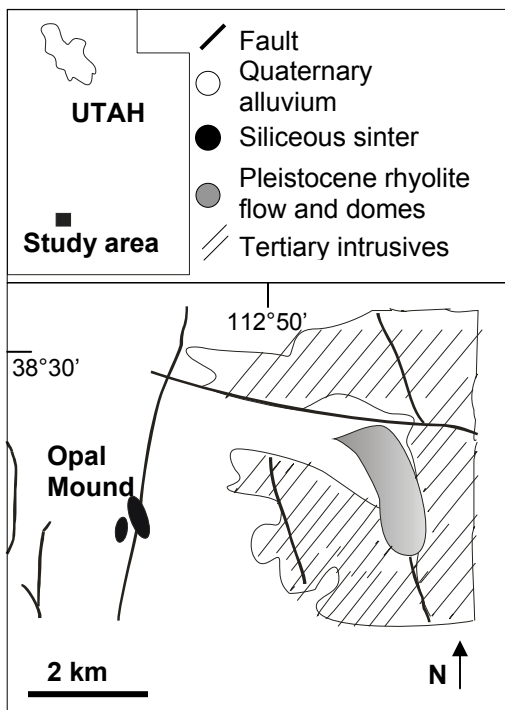


Figure 1 - Location of Opal Mound, Utah.

3. SAMPLE OCCURRENCE

Forty-eight sub-samples from 25 sinter samples collected at the Opal Mound were studied. These samples represent vent, near-vent, middle and distal apron slope environments. White sinter occurs along the crest of the Opal Mound ridge, in vent and near-vent locations; pale coloured sinter is from the middle apron slopes and brightly coloured sinter occurs on the distal slopes. Distal slopes consist of porous indurated and vitreous sinter; whereas, all other sinter samples are vitreous.

4. METHODS

The structural state of the siliceous sinter was measured by its degree of lattice order, following the X-ray Powder Diffraction (XRPD) techniques of Herdianita *et al.* (2000b). The band width at half maximum peak height (FWHM) was used to determine the degree of lattice order, or mineralogical maturation, of the silica structure. A narrowing and sharpening of the XRPD broadband occurs with diagenesis or silica phase maturation.

Sinter microscale features and textures were examined using optical and Scanning Electron Microscopy (SEM). Operating conditions are reported in Lynne *et al.* (2003).

A Renishaw Raman 1000 laser microprobe system was used to detect moganite. Data were collected using a solid state diode red laser set at 785 nm and 25 mW with a 1200 litre/minute diffraction grating

and cosmic ray inhibitor. Spectra were collected with a slit of 100 μm and an integration time of 10 seconds under 100 % power. The Raman was calibrated with calcite (1085 cm^{-1} peak) and silicon (520 cm^{-1} peak).

Two samples were ^{14}C dated by AMS at the Rafter Radiocarbon Laboratory, Institute of Geological and Nuclear Sciences Ltd, Lower Hutt, New Zealand. Details of this technique are described in Lynne *et al.* (2003).

5. RESULTS

Opal Mound siliceous sinter preserves the transformation from opal-A to quartz (Fig. 2). The XRPD analysis indicates that the white, vitreous sinter consists of opal-C and quartz silica phases. Pale coloured, mid-slope sinter comprises opal-CT, and brightly coloured distal-apron sinter contains opal-A. Erosion along the crest of the mound has exposed two vents 15 m apart. The northernmost vent is infilled with white vitreous sinter whereas the southernmost vent consists of porous indurated sinter. Opal Mound preserves an entire diagenetic continuum for silica minerals so that incremental mineralogic and morphologic steps during diagenesis can be traced across the deposit. Diagenesis occurs both gradually and gradationally, and each step is clearly recognisable by distinct morphological and mineralogical characteristics. These sinters record a range of silica phase maturation states. Two end members produced FWHM values of $7.70 \text{ }^\circ 2\theta$ (1.36 \AA) for opal-A and $0.15 \text{ }^\circ 2\theta$ (0.03 \AA) for quartz (Table 1).

Table 1 - XRPD silica phases at Opal Mound

| No. of samples | Range of FWHM values ($^\circ 2\theta/\text{\AA}$) | Silica Phase |
|----------------|--|----------------|
| 20 | 7.70-6.45/1.36-1.16 | Opal-A |
| 10 | 5.8-2.7/1.06-0.51 | Opal-A/CT |
| 5 | 2.30-1.05/0.44-0.20 | Opal-CT+quartz |
| 3 | 0.6-0.2/0.12-0.04 | Opal-C+quartz |
| 10 | 0.4-0.15/0.06-0.03 | Quartz |

A morphological pattern emerges of silica particle size changes during diagenesis, where particles grow from nanoscale to micron scale twice, with nanostructures aligning and merging to form larger features in each case (Fig. 3). The morphological-mineralogical sequence of events is outlined as follows. Initially, smooth opal-A spheres (Fig. 3A), transform into 200 nm diameter, nanospheres which subsequently align themselves into 1 μm long groups of incipient blades (Fig. 3B). These oriented nanospheres then transform into jagged bladed structures (Fig. 3C), eventually forming sharp

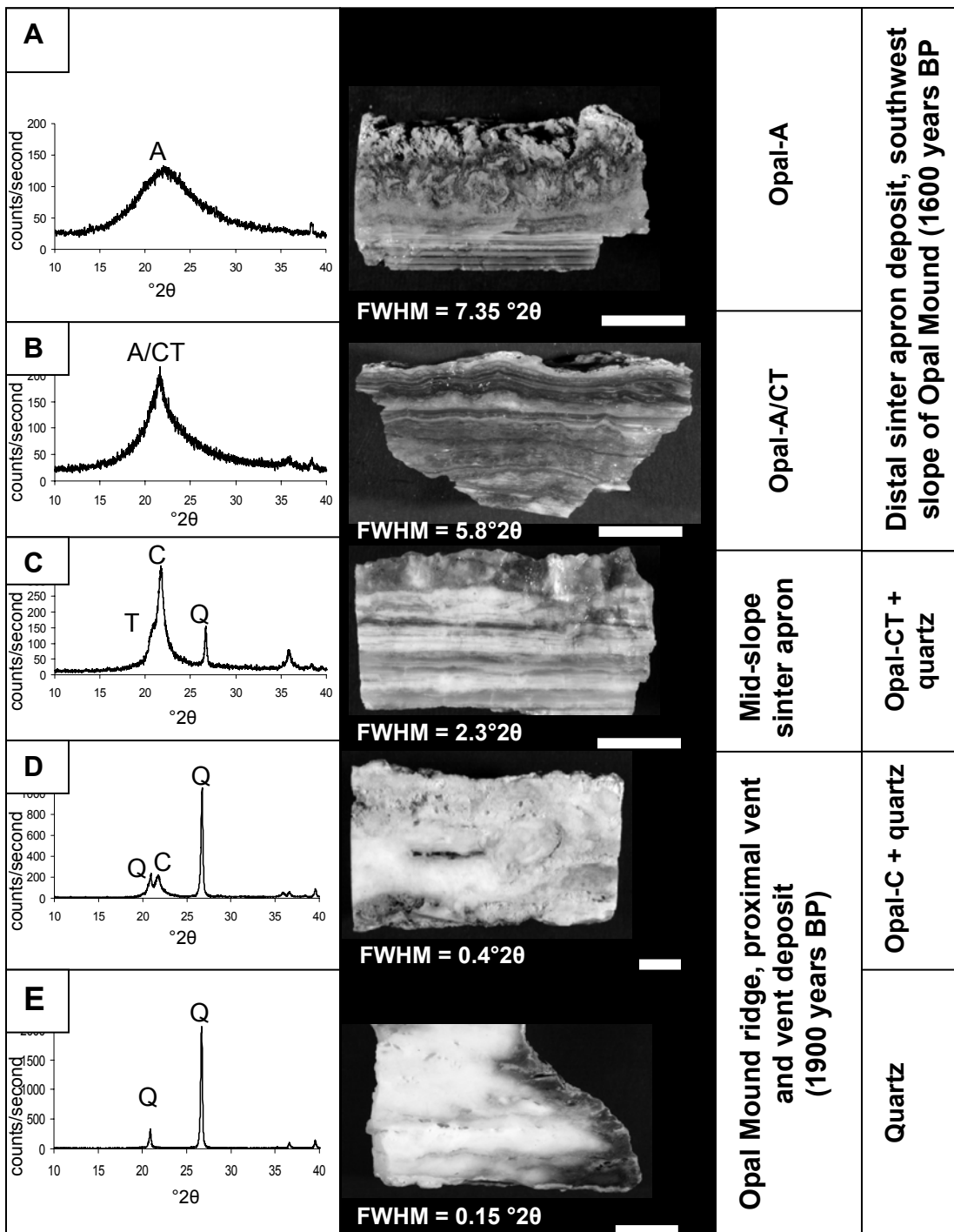


Figure 2 - XRPD traces, macrottextures and spatial context of opal-A to quartz diagenesis at Opal Mound. All scale bars = 10 mm. (A) Opal-A, located on distal apron slopes. (B) Opal-A/CT, located on distal apron slopes. (C) Opal-CT + quartz, representative of mid-slope sinter apron. (D) Opal-C + quartz, proximal vent location from Opal Mound ridge. (E) Quartz, from near-vent location, Opal Mound ridge.

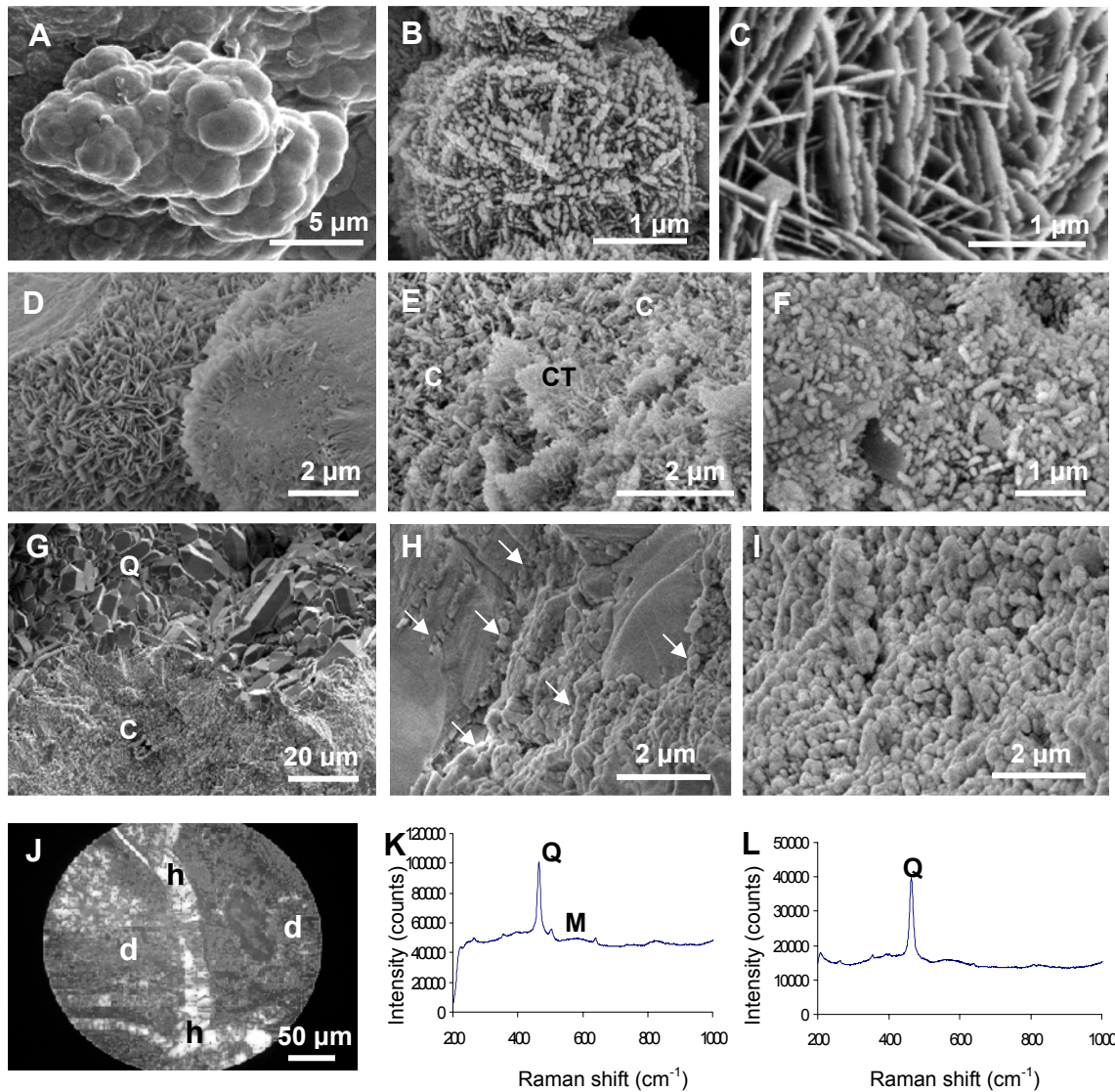


Figure 3 - Microstructural and compositional features accompanying the opal-A to quartz silica phase transition in sinter from Opal Mound, including micron-scale morphological transitions, quartz veining and moganite detection. (A) Botryoidal cluster of opal-A spheres with smooth surfaces. (B) Aligned opal-A/CT nanospheres, (200 nm diameter), within an incipient lepisphere (3.3 μm diameter). (C) Early formed opal-CT lepispheres reveal jagged upper edges of merged nanospheres. (D) Typical sharply bladed opal-CT lepispheres. (E) Remnant opal-CT bladed lepispheres (CT) in a groundmass of opal-C (C). (F) Opal-C nano-lozenge structures (200 nm long). (G) Diagenetic quartz crystals (Q), growing parallel to the surface from a groundmass of opal-C (C). (H) Diagenetic quartz crystals, parallel to sinter surface, reveals bands of equant, blocky nanostructures (200 nm diameter) around their bases (arrows). (I) Detail of bands of blocky textures parallel to sinter surface, which are representative of early diagenetic quartz crystal growth. (J) Thin section image, crossed polarised light, reveals a groundmass of diagenetic quartz (d) with secondary quartz infilling veins (h). (K) Raman microprobe scan detected quartz (Q) and moganite (M) in the groundmass (d of J). (L) Raman microprobe scan within quartz vein (h of J) detected quartz (Q) only.

blades of typical opal-CT lepispheres (Fig. 3D). The opal-CT to opal-C transformation involves the breakdown of blades into 200 nm diameter nanolozenge (Fig. 3E, F). Diagenesis continues as the lozenges restructure themselves into nano-sized equant blocks (Fig. 3G-I). Finally the blocks serve as the bases for growing quartz crystals (Fig. 3I), where they become incorporated into the emerging crystal. Two generations of quartz have been recognised at Opal Mound, diagenetic quartz and vein quartz. Diagenetic quartz forms from the transformation of opal-C nanostructures in the groundmass and grows parallel to the sinter surface. Moganite was detected within the paragenetic sequence leading to diagenetic quartz (Fig. 3J, K), but was not found in vein quartz, which lacks opal-C nanostructures. Vein quartz grows normal to surfaces infilling cross-cutting veins and fractures (Fig. 3J, L).

6. CONCLUSIONS

Opal Mound contains the entire diagenetic sequence of silica mineral phase transformations within a single sinter deposit. The formation of diagenetic quartz after only 1900 years demonstrates that silica phase changes can occur rapidly. Rodgers *et al.* (2004) reported accelerated diagenesis for silica residue and attributed it to the effect of heat from acidic steam condensate during its formation. The injection of hydrothermal fluids could have heated the sinter at Opal Mound by conductive heat transfer, thereby accelerating the rate of diagenesis. The transformation of Opal-A to quartz at Opal Mound reveals a morphological pattern of silica particle sizes that enlarge-decrease-enlarge-decrease (alternating nano- to micron-scales) as maturation proceeds from opal-A to opal-CT to opal-C to moganite to quartz.

7. ACKNOWLEDGEMENTS

This research was funded by the Foundation for Research of Science and Technology, on behalf of the Ministry of Education, and Auckland University. Funds for J. Moore were provided by the U.S. Department of Energy undercontract DE-FG3600 ID13891. We thank L. Cotterall, A. Arcila, R. Sims, C. Hobbs and D. Langton for technical support.

8. REFERENCES

Campbell, K.A., Sannazzaro, K., Rodgers, K.A., Herdianita, N.R. and Browne, P.R.L. (2001). Sedimentary facies and mineralogy of the Late Pleistocene Umukuri silica sinter, Taupo Volcanic Zone, New Zealand. *Journal of Sedimentary Research*, Vol. 71, 727-746.

Capuano, R.M. and Cole, D.R. (1982). Fluid-mineral equilibria in high temperature geothermal systems. The Roosevelt Hot Springs geothermal system, Utah. *Geochimica et Cosmochimica Acta*, Vol. 46, 1353-1364.

Fournier, R.O. and Rowe, J.J. (1966). Estimation of underground temperatures from the silica content of water from hot springs and steam wells. *American Journal of Science*, Vol. 264, 685-697.

Herdianita, N.R., Browne, P.R.L., Rodgers, K.A. and Campbell, K.A. (2000a). Mineralogical and textural changes accompanying ageing of silica sinter. *Mineralium Deposita*, Vol. 35, 48-62.

Herdianita, N.R., Rodgers, K.A. and Browne, P.R.L. (2000b). Routine instrumental procedures to characterise the mineralogy of modern and ancient silica sinters. *Geothermics*, Vol. 29, 65-81.

Lynne, B.Y. and Campbell, K.A. (2003). Diagenetic transformations (opal-A to quartz) of low- and mid-temperature microbial textures in siliceous hot-spring deposits, Taupo Volcanic Zone, New Zealand. *Canadian Journal of Earth Sciences*, Vol. 40, number 11, 1679-1696.

Lynne, B.Y., Moore, J., Browne, P.R.L. and Campbell, K.A. (2003). Age and mineralogy of the Steamboat Springs silica sinter deposit, Nevada, U.S.A: A preliminary report of core SNLG 87-29. *Proceedings 25th NZ Geothermal Workshop*, 65-70.

Lynne, B.Y. and Campbell, K.A. (2004). Morphologic and mineralogic transitions from opal-A to opal-CT in low-temperature siliceous sinter diagenesis, Taupo Volcanic Zone, New Zealand. *Journal of Sedimentary Research*, Vol. 74, number 4, 561-579.

Moore, J. M. and Nielson, D.L. (1994). An overview of the geology and geochemistry of the Roosevelt Hot Springs geothermal system, Utah. *Utah Geological Association Publication*, 23, 25-36.

Mundorff, J. C. (1970). Major thermal springs of Utah. *Utah Geological and Mineral Survey Water Resources Bulletin*, 13, 1-60.

Nielson, D.L., Sibbet, B.S., McKinney, D.B., Hulen, J.B., Moore, J.N. and Samberg, S.M. (1978). Geology of Roosevelt Hot Springs KGRA, Beaver Country, Utah. *University of Utah Research Institute, Earth Science Laboratory Report 12*, 1-120.

Rodgers, K.A., Browne, P.R.L., Buddle, T.F., Cook, K.L., Greatrex, R.A., Hampton, W.A., Herdianita, N.R., Holland, G.R., Lynne, B.Y., Martin, R., Newton, Z. Pastars, D., Sannazarro, K.L. and Teece, C.I.A. (2004). Silica phases in sinters and residues from geothermal fields of New Zealand. *Earth Science Reviews*, Vol. 66, 1-61.

Smith, D.K. (1998). Evaluation of the detectability and quantification of respirable crystalline silica by x-ray powder diffraction. *Powder Diffraction*, Vol. 12(4), 200-227.

White, D.E., Thompson, G.A. and Sandberg, C.H. (1964). Rocks, structure, and geologic history of Steamboat Springs thermal area, Washoe Country, Nevada, *U.S. Geological Survey Professional Paper* 458-B, 63p.